SAND2007-0455P

Project no. 506604

HyICE

Optimization of a Hydrogen Powered
Internal Combustion Engine

Integrated Project

Priority 6.2.ii

Sustainable Surface Transport

LES of mixing and combustion for direct-injection operation

Deliverable D4.3.G

Due date of deliverable: 31.12.2007
Submitted to internal reviewers:
Actual submission date: 25.01.2007

Start date of project: 05.01.2004 Duration: 36 months

Sandia National Laboratories

Version 0.1

Project co-funded by the European Commission within the Sixth Framework Programme (2002-2006)		
Dissemination Level		
PU	Public	
PP	Restricted to other programme participants (including the Commission Services)	X
RE	Restricted to a group specified by the consortium (including the Commission Services)	
CO	Confidential, only for members of the consortium (including the Commission Services)	

Authors

Joseph C. Oefelein, Sandia National Laboratories

Phone +925-294-2648

fax +925-462-2595

e-mail oefelei@sandia.gov

Project Co-ordinator

Hans-Christian Fickel

BMW Forschung und Technik GmbH

phone +49 89 382 68395

fax +40 89 382 70 68395

e-mail hans.fickel@bmw.de

Partners

BMW Forschung und Technik GmbH
Ford Forschungszentrum Aachen GmbH
Volvo Technology Corporation
MAN Nutzfahrzeuge AG
Hoerbiger Valve Tec GmbH
Institut Français du Pétrole
Technische Universität Graz
Universität der Bundeswehr München
Mecel AB
Irion Management Consulting GmbH
ANSYS Germany GmbH

Revision chart and history log

Version	Date	Reason
0.1	25.01.2007	First draft by J. Oefelein

Table of contents

Authors iii
Project Co-ordinator iii
Partners iii
Revision chart and history log iv
Table of contents v
Summary 1
1 Introduction 2
2 Approach 3
2.1 Theoretical Framework 3
2.2 Numerical Framework 5
2.3 Modeling Approach 6
2.4 Target Validation Cases 7
3 Results 9
3.1 Detailed Thermodynamics and Transport 9
3.2 Validation of the O'Conaire et al. H_2 – Air Mechanism 11
3.3 Tabulated Combustion Closure Based on LEM 13
4 Conclusions 15
References 16

Summary

This research combines a unique high-fidelity simulation capability based on the Large Eddy Simulation (LES) technique with the Advanced Combustion Engine R&D activities at Sandia National Laboratories. The objective is to use high-fidelity science-based simulations in a manner that directly complements select optical engine experiments. Each of the proposed tasks requires considerable high-level expertise, labor, and computational resources. They significantly exceed the time and resources available in industry and academia and are consistent with a National Laboratory's role of using high-performance computing to enable fundamental exploration of complex combustion phenomena. The simulations are being carried out using a highly specialized state-of-the-art flow solver. This software provides a unique enabling capability well suited for the proposed set of tasks.

Currently, we are focused on the application of LES to perform high-fidelity calculations of direct-injection mixing and combustion processes in the optically accessible hydrogen-fueled IC-engine developed by White et al. at Sandia National Laboratories (see deliverable D4.3.F "Final results of mixture formation and combustion in an optical engine"). Prerequisite tasks to achieve this goal are to establish the ability to handle 1) detailed thermodynamics and transport for stratified mixtures in reacting hydrogen-air systems (including cases when the hydrogen is in a cryogenic state), 2) detailed hydrogen-air chemistry over the relevant range of pressures and temperatures, and 3) in-cylinder turbulence-chemistry interactions through specification of an appropriate combustion closure. These three items are the topic of this report.

1 Introduction

In theory, a direct-injection hydrogen-fueled IC-engine (DI-H2ICE) can provide 15% more horsepower than the identical engine fueled with gasoline. The challenge, however, is that in-cylinder injection requires that hydrogen and air mix in a very short time (approximately 4 ms at 5000 rpm). Since mixture formation at the start of combustion is critical to engine performance and emissions, a fundamental understanding of the effects and optimization of in-cylinder hydrogen-air mixture formation is necessary before commercialization is possible. The collaborative experimental-numerical research being conducted by White and Oefelein are designed to systematically address these issues. Experimental results are complemented with a closely coupled set of numerical calculations using LES. These simulations are conducted using a highly specialized massively parallel flow solver designed to treat the turbulent reacting flows in IC-engines.

Our objective is to perform detailed LES calculations of the full optical engine geometry in a manner that is directly synchronized with the experimental research. Tasks associated with this objective include 1) development of advanced subgrid-scale (SGS) models for time-accurate treatment of direct-injection mixing and combustion of hydrogen-air processes, 2) systematic verification and validation of the coupled system of models, and 3) joint complementary analysis of key in-cylinder engine processes with emphasis placed on three-dimensional effects. The type of calculations performed here are quite different than those performed in industry. Each case requires significant levels of labor and computational resources. A single case can take on the order of 500,000 CPU hours on contemporary supercomputer platforms. Thus, a high level of effort goes into preliminary setup of the runs.

Our emphasis to date has been placed on the development of a comprehensive modeling framework for treatment of turbulent hydrogen-air mixing and combustion. We have developed a detailed property evaluation scheme capable of handling arbitrary hydrocarbon mixtures, including hydrogen, oxygen and nitrogen, over a wide range of conditions (including cryogenic states). We have coupled this to the newest state-of-the-art chemical kinetics mechanism for hydrogen-air systems and have verified the accuracy of this mechanism over the relevant range of pressures and temperatures observed in the engine. Using these tools we have also established an efficient tabulated combustion closure based on the Linear Eddy Model (LEM) of Kerstein et al. (see Kerstein 1988 - 1992). We are in the process of validating the coupled system of models over the envelope of conditions observed in both the current experiment, and also for conditions where the hydrogen is injected at cryogenic conditions.

2 Approach

Application of the LES technique provides the formal ability to treat the full range of multidimensional time and length scales that exist in turbulent reacting flows in a computationally feasible manner. The large energetic scales are resolved directly. The small “subgrid-scales” are modeled. This provides a way to simulate the complex multiple-time multiple-length scale coupling between processes in a time-accurate manner and facilitates analysis of all dynamic processes simultaneously. Treating the full range of scales is a critical requirement since phenomenological processes are inherently coupled through a cascade of nonlinear interactions. The baseline theoretical-numerical framework employed at the CRF combines a general treatment of the governing conservation and state equations with state-of-the-art numerical algorithms and massively-parallel programming paradigms. Recent results and detailed formulations are given by Oefelein (2005, 2006a-c) and Oefelein et al. 2006.

2.1 Theoretical Framework

The approach is enabled through a unique theoretical-numerical framework developed over the last decade. This framework solves the fully coupled conservation equations of mass, momentum, total-energy and species for complex chemically reacting flows in complex geometries. The numerical formulation treats the fully-coupled compressible form of the conservation equations but can be evaluated in the incompressible limit. The theoretical framework handles both multicomponent and mixture-averaged systems, with a generalized treatment of the equation of state, thermodynamics, and transport processes. It can accommodate high-pressure real-gas/liquid phenomena, multiple-scalar mixing processes, finite-rate chemical kinetics, and multiphase phenomena in a fully coupled manner. For LES applications, the instantaneous conservation equations are filtered and models are applied to account for the subgrid-scale (SGS) mass, momentum and energy transport processes. The baseline SGS closure is obtained using the mixed dynamic Smagorinsky model by combining the models of Erlebacher et al. (1992) and Speziale (1985) with the dynamic modeling procedure (Germano et al. 1991, Moin et al. 1991, Lilly 1992) and the Smagorinsky (1963) eddy viscosity model. There are no tuned constants employed anywhere in the closure.

The baseline formulation accommodates a generalized treatment of the equation of state, thermodynamics, transport processes, and chemical kinetics for the full multicomponent system. No assumptions are made regarding the ideality of the mixture state. For LES applications the instantaneous conservation equations are filtered yielding:

- Mass:

$$\frac{\partial}{\partial t}(\theta\overline{\rho}) + \nabla\cdot(\theta\overline{\rho}\tilde{\mathbf{u}}) = \overline{\dot{\rho}}_s \tag{1}$$

- Momentum:

$$\frac{\partial}{\partial t}(\theta\overline{\rho}\tilde{\mathbf{u}}) + \nabla\cdot\left[\theta\left(\overline{\rho}\tilde{\mathbf{u}}\otimes\tilde{\mathbf{u}} + \frac{\mathcal{P}}{M^2}\mathbf{I}\right)\right] = \nabla\cdot(\theta\vec{\vec{\mathcal{T}}}) + \overline{\dot{\mathbf{F}}}_s \tag{2}$$

- Total Energy:

$$\frac{\partial}{\partial t}(\theta\overline{\rho}\tilde{e}_t) + \nabla\cdot[\theta(\overline{\rho}\tilde{e}_t + \mathcal{P})\tilde{\mathbf{u}}] = \nabla\cdot\left[\theta\left(\vec{\mathcal{Q}}_e + M^2(\vec{\vec{\mathcal{T}}}\cdot\tilde{\mathbf{u}})\right)\right] + \theta\overline{\dot{Q}}_e + \overline{\dot{Q}}_s \tag{3}$$

- Species:

$$\frac{\partial}{\partial t}(\theta\overline{\rho}\tilde{Y}_i) + \nabla\cdot(\theta\overline{\rho}\tilde{Y}_i\tilde{\mathbf{u}}) = \nabla\cdot(\theta\vec{\mathcal{S}}_i) + \theta\overline{\dot{\omega}}_i + \overline{\dot{\omega}}_{s_i} \tag{4}$$

• Spray Source Terms • Composite Stresses/Fluxes • Chemical Source Terms

The terms highlighted in red represent the filtered void fraction and spray source terms, which account for exchange of mass, momentum, total energy and species, respectively. The terms highlighted in green represent respective composite (i.e., molecular plus SGS) stresses and fluxes. The terms highlighted in blue represent the filtered energy and species source terms.

The baseline SGS closure is obtained using the “mixed” dynamic Smagorinsky model by combining the models proposed by Erlebacher, Hussaini, Speziale and Zang (1992) and Speziale (1985) with the dynamic modeling procedure. The composite stresses and fluxes in Eqs. (1)-(4) are given as

$$\vec{\vec{\mathcal{T}}} = (\mu_t+\mu)\frac{1}{Re}\left[-\frac{2}{3}(\nabla\cdot\tilde{\mathbf{u}})\mathbf{I} + \left(\nabla\tilde{\mathbf{u}} + \nabla\tilde{\mathbf{u}}^T\right)\right] - \overline{\rho}\left(\widetilde{\mathbf{u}\otimes\mathbf{u}} - \tilde{\mathbf{u}}\otimes\tilde{\mathbf{u}}\right), \tag{5}$$

$$\vec{\mathcal{Q}}_e = \left(\frac{\mu_t}{Pr_t} + \frac{\mu}{Pr}\right)\frac{1}{Re}\nabla\tilde{h} + \sum_{i=1}^{N}\tilde{h}_i\vec{\mathcal{S}}_i - \overline{\rho}\left(\widetilde{h\tilde{\mathbf{u}}} - \tilde{h}\tilde{\mathbf{u}}\right), \text{ and} \tag{6}$$

$$\vec{\mathcal{S}}_i = \left(\frac{\mu_t}{Sc_{t_i}} + \frac{\mu}{Sc_i}\right)\frac{1}{Re}\nabla\tilde{Y}_i - \overline{\rho}\left(\widetilde{Y_i\tilde{\mathbf{u}}} - \tilde{Y}_i\tilde{\mathbf{u}}\right). \tag{7}$$

The term μ_t represents the SGS eddy viscosity, given by

$$\mu_t = \overline{\rho}C_R\Delta^2\Pi_{\tilde{\mathbf{S}}}^{\frac{1}{2}}, \tag{8}$$

where

$$\Pi_{\tilde{\mathbf{S}}} = \tilde{\mathbf{S}}:\tilde{\mathbf{S}}, \text{ and } \tilde{\mathbf{S}} = \frac{1}{2}\left(\nabla\tilde{\mathbf{u}} + \nabla\tilde{\mathbf{u}}^T\right). \tag{9}$$

The terms C_R, Pr_t, and Sc_{ti} represent the Smagorinsky, SGS-Prandtl and SGS-Schmidt numbers and are evaluated dynamically as functions of space and time. The overall model includes the Leonard and cross-term stresses and provides a Favre averaged generalization of the Smagorinsky eddy viscosity model coupled with gradient diffusion models that simulate SGS mass and energy transport processes.

2.2 Numerical Framework

The numerical formulation treats the fully-coupled compressible conservation equations but can be evaluated in the incompressible limit. Thus, incompressibility is treated as a limiting extreme of the more general compressible equation set given by Eqs. (1)-(4). A unique dual-time multistage scheme is employed with a generalized preconditioning methodology that optimally treats convective, diffusive, geometric, and source term anomalies in a unified manner. The spatial scheme employs a staggered methodology in generalized curvilinear coordinates that provides “non-dissipative” spectrally clean damping characteristics and discrete conservation of mass, momentum and total-energy. This is a critically important feature for LES. The differencing methodology also includes appropriate switches to handle shocks, detonations, flame-fronts and/or contact discontinuities in a manner appropriate for LES.

The baseline scheme provides a fully implicit time advancement using a fully explicit multistage scheme in pseudo-time. The implicit formulation is A-stable, which allows one to set the physical-time step based solely on accuracy considerations. It accommodates any arbitrary equation of state, handles thermodynamic non-idealities and transport anomalies over a wide range of conditions typically encountered in contemporary propulsion and power systems, and provides full thermophysical coupling over a wide range of conditions. A Lagrangian-Eulerian formulation is employed to accommodate particulates, sprays, or Lagrangian based combustion models, with full coupling applied between the two systems. The Lagrangian solver can accommodate both particles and parcel methods and employs asynchronous multiple time-scale integration to efficiently account for time-history effects.

The algorithm has been optimized to provide excellent parallel scalability attributes using distributed multiblock domain decomposition with a generalized connectivity scheme. Distributed-memory message-passing is performed using MPI. It accommodates complex geometric features and time-varying meshes with generalized hexahedral cells while maintaining the accuracy of structured spatial stencils. The LES software package has been ported and run on all contemporary massively-parallel hardware, including those built by the Department of Energy (DOE) under the Advanced Simulation and Computing Initiative (ASCI) (www.llnl.gov/asci/platforms), and those housed by the Pittsburgh Supercomputing Center (www.psc.edu), NASA, DOD and at Sandia National Laboratories, including SGI Origin’s and commodity PC clusters (www.cs.sandia.gov/cplant). The basic method is well suited for massively-parallel computations and maintains highly efficient fine-grain scalability attributes.

2.3 Modeling Approach

Our combustion modeling approach facilitates direct treatment of turbulence-chemistry interactions and multiple-scalar mixing processes without the use of tuned model constants. The systematic development and validation of this approach is currently a major focal point. Given the large body of activity in this area, our goal is to be complementary, not redundant, and use the unique features of our theoretical-numerical framework to provide an enhanced level of understanding. We are currently investigating two new modeling approaches. The first employs a stochastic reconstruction methodology that treats detailed chemistry directly within the LES formalism. This model is “science-based” in that it facilitates direct treatment of turbulence-chemistry interactions and multiple-scalar mixing in a manner consistent with the application of DNS. The second employs a related subset of fundamental assumptions but is “engineering-based” and employs a tabulated combustion closure based on LEM. Given the nature of the combustion processes of interest here, our current focal point is the tabulated LEM model. This model is potentially an order of magnitude faster.

The tabulated approach is a new implementation of LEM with many potentially beneficial attributes. Given our experience with this model (and collaboration with A. Kerstein), we have begun to investigate the merits of a tabulated combustion closure based on LEM. Turbulent reactive closures that relate the statistics of the chemical species to those of a conserved scalar such as mixture fraction have been moderately successful in representing turbulence-chemistry interactions under certain conditions. Laminar flamelet modeling, for example, attempts to capture the coupling between turbulence and chemistry by constructing SGS models for the PDF of mixture fraction and scalar dissipation rate. A current difficulty with the flamelet approach is that it cannot predict local extinction and re-ignition behavior reliably. The primary reason is that the dependence of the scalar dissipation rate on mixture fraction is not necessarily unique under these conditions. Conceptually, LEM can circumvent these difficulties by embedding the dependence within the model framework. A one-dimensional reaction-diffusion equation is solved that resolves processes over all the scales of turbulence and chemistry. Molecular diffusion and reactive source terms are computed explicitly. Advection is modeled by a stochastic mapping procedure that satisfies the three-dimensional inertial range scaling laws.

Given these advantages, we have proposed a new tabulation approach that is analogous to mapping of “turbulent-flamlets.” The turbulence closure is embedded as an integral part of the table. Thermo-chemical state libraries are constructed in a manner directly analogous to the conventional flamelet-library approach. A unique difference, however, is that LEM simulates instantaneous realizations of the flow as a function of both the resolved and the unresolved strain-rate. Hence, ensemble averaged solutions of the LEM field can be directly parameterized and tabulated based on filtered values of mixture fraction, scalar dissipation rate, and turbulent Reynolds number. This eliminates the need to introduce additional models to link filtered quantities with instantaneous

quantities. We are currently performing companion studies using both tabulated LEM and the stochastic reconstruction model.

2.4 Target Validation Cases

Validation case studies include both “out-of-engine” and “in-cylinder” calculations. The culmination of studies being considered are a direct extension of joint activities currently underway in the Turbulent Combustion Laboratory (TCL) and the optically accessible Internal Combustion Engine (ICE) Laboratories at the CRF. These activities involve significant domestic and international collaborations. Both the TCL and ICE Laboratories were designed to accelerate the development of predictive combustion models by providing the next level of experiments needed to extend our fundamental understanding of turbulent combustion and to expand the basis for rigorous model validation. Research conducted in the TCL is focused exclusively on fundamental flame configurations at moderately high Reynolds numbers. Research conducted in the ICE Laboratories provides a natural extension to the more complex issues associated with in-cylinder turbulence-chemistry interactions in ICE’s. Joint research is being conducted in collaboration with researchers involved with the International Workshop on Measurement and Computation of Turbulent Nonpremixed Flames (i.e., the so-called “TNF Workshop” founded by Barlow 1996-2006, www.ca.sandia.gov/TNF).

In addition to the TNF Workshop flame series, our focal point has been the CRF optical DI-H2ICE configuration of White. The baseline geometry and grid are shown in Fig. 1. The corresponding valve and spark timing profiles are shown in Fig. 2. We have now refined the grid to include the port and valve configuration that identically matches the experimental geometry. The refitted direct-injection engine configuration employs a flat-piston with a four-valve pent-roof head and has been designed to handle a range of compression ratios from 9.5 to 12.5. Here, the ports have been removed to show details in the vicinity of the valves. The valve topology is shown in the images at 360 and 432 CAD. The multiblock grid topology is shown in the image at 540 CAD. The black lines highlight a typical generalized multiblock decomposition (137 blocks for this case), where one block per processor is run on a distributed massively parallel computer platform. Our baseline case is being performed using 3.2-million cells. Subsequent calculations will approach 10-million cells. In addition to advanced software, performing the detailed calculations requires significant computational resources. Each calculation requires on the order of 100 to 500-thousand CPU hours.

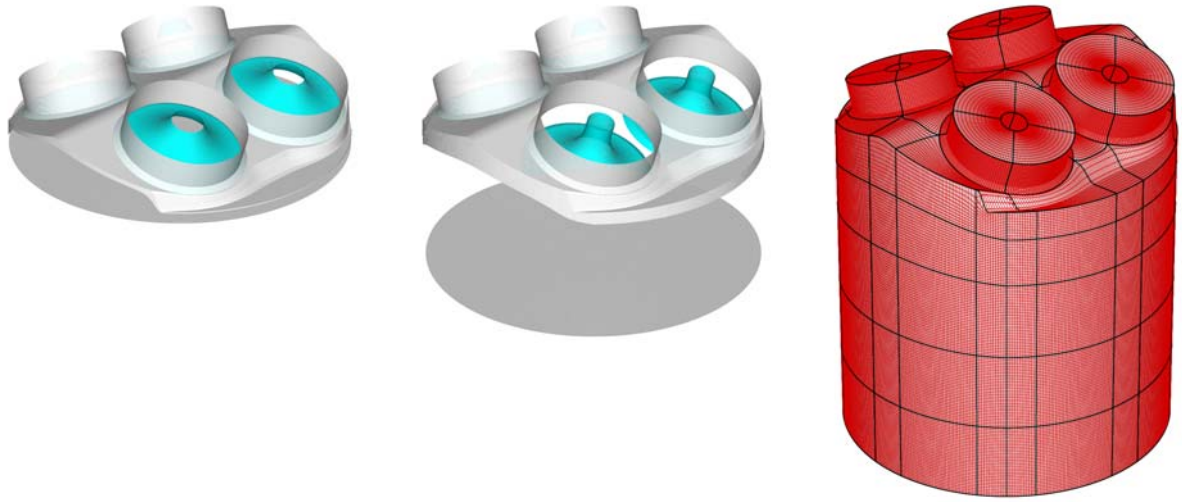

Figure 1: Generalized time-varying multiblock grid at 360, 432, and 540 CAD (intake stroke) used for LES of the CRF DI-H2ICE engine (3-million cells, 137 blocks, ports removed from images).

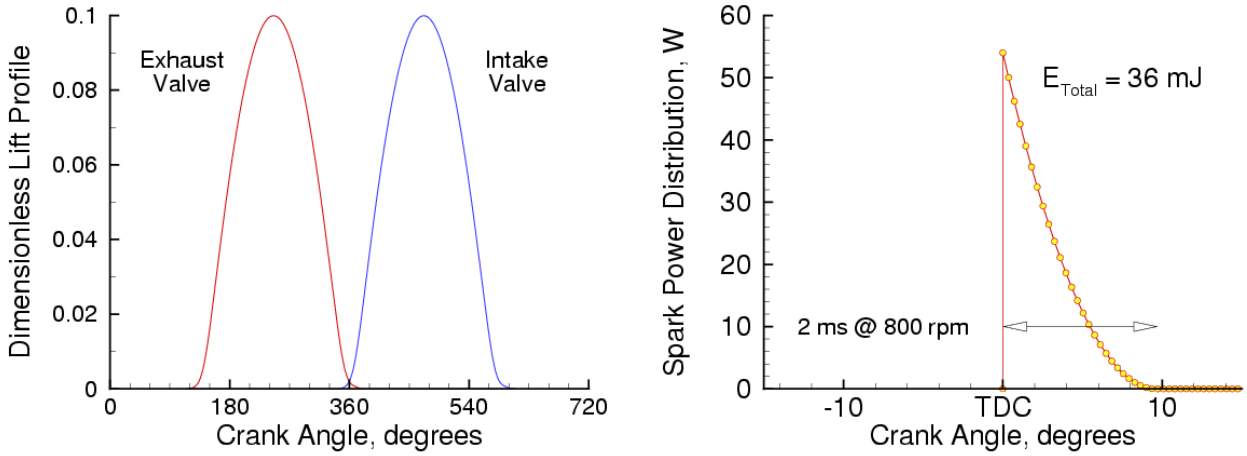

Figure 2: Valve and spark timing profiles.

3 Results

Our current emphasis has been on the application of LES to direct-injection mixing and combustion processes in the optically accessible hydrogen-fueled IC-engine developed by White et al. (see deliverable D4.3.F “Final results of mixture formation and combustion in an optical engine”). There are several prerequisite tasks required to achieve this goal. First, we established and verified our ability to handle detailed thermodynamics and transport for stratified mixtures in reacting hydrogen-air systems (including cases when the hydrogen is in a cryogenic state). Second, we performed a series of studies to validate the newest state-of-the-art finite-rate mechanism for hydrogen-air chemistry over the relevant range of pressures and temperatures. Last, we have combined these validated capabilities into a comprehensive combustion closure model based on the tabulated LEM approach. In the sections below (3.1 – 3.3), we provide an overview of results from these three prerequisite studies.

3.1 Detailed Thermodynamics and Transport

The property evaluation scheme we have developed is designed to account for detailed thermodynamics and transport over a wide range of pressures and temperatures (including nonideal, liquid and cryogenic regimes). The scheme is comprehensive and intricate; thus, only a skeletal description can be given here. The extended corresponding states model (Leland and Chappelear 1968, Rowlinson and Watson 1969) is employed with both the Benedict-Webb-Rubin (BWR) equation of state and cubic equations of state. These provide highly accurate estimates for the p-v-T behavior of the inherent dense multicomponent mixtures. Use of modified BWR equations of state in conjunction with the extended corresponding states principle has been shown to provide consistently accurate results over the widest range of pressures, temperatures and mixture states, especially at near-critical conditions.

A major disadvantage of BWR equations is that they are not computationally efficient. Cubic equations of state can be less accurate, especially for mixtures at near-critical or saturated conditions, but are computationally efficient. Experience has shown that both the Soave-Redlich-Kwong (SRK) and Peng-Robinson (PR) equations, when used in conjunction with the corresponding states principle, can give accurate results over the range of pressures, temperatures and mixture states of interest in this study. The SRK coefficients are fit to vapor pressure data and are thus more suitable for conditions when the reduced temperature is less than one. The PR coefficients, on the other hand, are more suitable for conditions when the reduced temperature is greater than one. Here the flow involves heat release, thus, the PR equation of state was used exclusively. A summary of the cubic equations of state and recommended constants is given by Reid et al. (1987; Chapter 3).

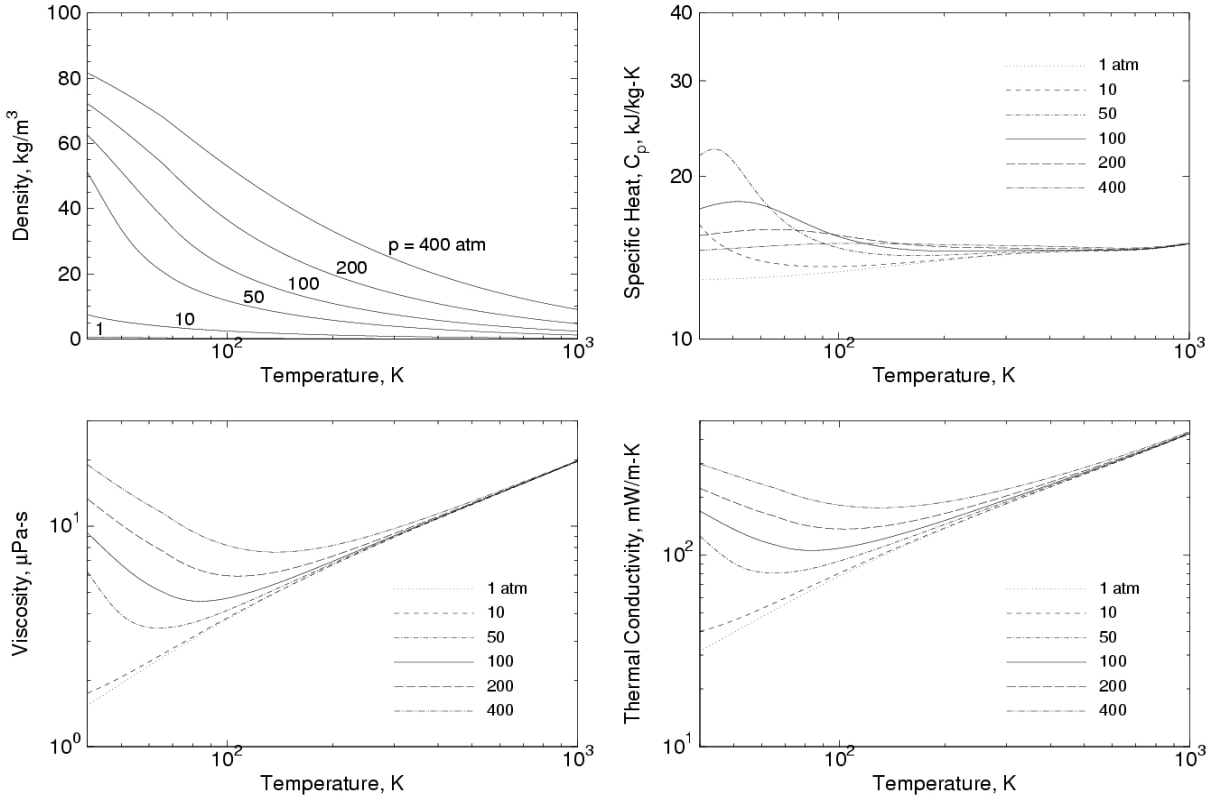

Figure 3: Thermophysical properties of hydrogen over the temperature range $40 \leq T \leq 1000$ and pressures of 1, 10, 50, 100, 200, and 400 atmospheres.

Having established an analytical representation for real mixture p-v-T behavior, the thermodynamic properties are obtained in two steps. First, component properties are combined at a fixed temperature using the extended corresponding states methodology to obtain the mixture state at a given reference pressure. A pressure correction is then applied using departure functions of the form given by Reid et al. (1987; Chapter 5). These functions are exact relations derived using the Maxwell relations and make full use of the p-v-T path dependencies dictated by the equation of state. Standard state properties are obtained using the databases developed by Gordon and McBride (1971) and Kee et al. (1990). Chemical potentials and fugacity coefficients are obtained in a manner similar to that outlined above.

Molecular transport properties are evaluated in an analogous manner. Viscosity and thermal conductivity are obtained using the extended corresponding states methodologies developed by Ely and Hanley (1981a, 1981b). Mass diffusion and thermal diffusion coefficients are obtained using the methodologies outlined by Bird et al. (1960) and Hirschfelder et al. (1964) in conjunction with the corresponding states methodology proposed by Takahashi (1974). The integrated package provides a numerically efficient way to calculate thermophysical properties on the fly for any arbitrary hydrocarbon. This is imperative for treatment of direct injection processes since the density of hydrogen is much lower than that of air. We have validated this package using the NIST database for the conditions of interest. Figure 3 shows representative results for hydrogen over a wide range of temperatures and pressures.

3.2 Validation of the O'Conaire et al. H_2 – Air Mechanism

Discussions with Professor J.-Y Chen (U. C. Berkeley) and Dr. Charlie Westbrook (LLNL) have provided a firm candidate for treatment of hydrogen-oxygen reactions at the pressures of interest here. This mechanism is described in the paper entitled "A Comprehensive Modeling Study of Hydrogen Oxidation" by O'Conaire, et al. (2004) and has been classified independently by both Chen and Westbrook as the most up to date and accurate. Thus, it supersedes the old "workhorse" 9 species, 17 step mechanism that was previously is in wide use. To establish our combustion closure, we have combined the property evaluation scheme described in section 3.1 with this mechanism and have run a series of opposed jet calculations to determine the accuracy and stiffness characteristics of this mechanism. Additionally, we have analyzed the flame structure produced by this mechanism to understand what the critical sensitivities are with respect to the fluid dynamic interactions.

A series of opposed jet simulations were performed to investigate issues related to the structure and chemical kinetics of gaseous hydrogen-oxygen flames at conditions similar to that expected in the optical DI-H2ICE configuration. Finite-rate hydrogen-oxygen kinetics were employed using the nine species (H_2, O_2, OH, H_2O, H, O, HO_2, H_2O_2, and N_2) mechanism optimized by O'Conaire et al. This mechanism has been tested over a range of pressures from 5 kPa to just under 10 MPa, and equivalence ratios from 0.2 to 6. Tests have validated the accuracy of the mechanism for predicting ignition delay times, flame speeds, and species composition. Sensitivity analysis has also shown which reactions dominate as a function of pressure, temperature and composition.

For use in our tabulated LEM closure, it is necessary to quantify the sensitivity of the mechanism over a wide range of strain-rates. The strain on the flame was adjusted by varying the fuel and oxidizer stream velocities over a range from 50 s^{-1} to 2000 s^{-1}. In all cases, the flame exhibits an extremely robust double-peaked reaction zone. The thickness of the reaction zone is inversely proportional to the level of strain. Results have been tabulated in the standard Chemkin format. Note that select subsets of these data can be tabulated in any format (depending on the solver) to provide appropriate libraries for both ignition and combustion. We can also generate standard flamelet libraries as a function of mixture fraction and the scalar dissipation rate, as requested.

We have performed these calculations to understand the baseline characteristics of the overall finite-rate mechanism at conditions similar to optical DI-H2ICE. At preheated conditions and elevated pressures (i.e., TDC), a robust flame structure is observed that is somewhat insensitive to the strain-rate. This is a favourable condition, which at the very least suggests that a flamelet type of approach can potentially be effective, both for ignition and producing a flame structure close to that given by the finite-rate mechanism. Figures 4 and 5 show the nominal temperature and mass fraction distribution that are produced as a function of mixture fraction. We expect these types of distributions near TDC. Here we show the structure for a strain-rate of 400 s^{-1}. There is no noticeable deviation in these profiles over the range of strain-rates from 50 s^{-1} to 2000 s^{-1}.

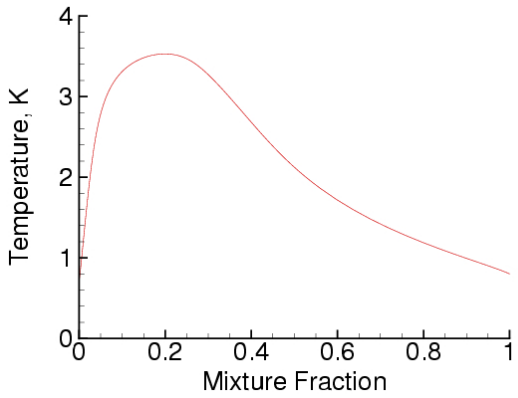

Figure 4: Temperature distribution as a function of mixture fraction for a strain-rate of 400 s^{-1}.

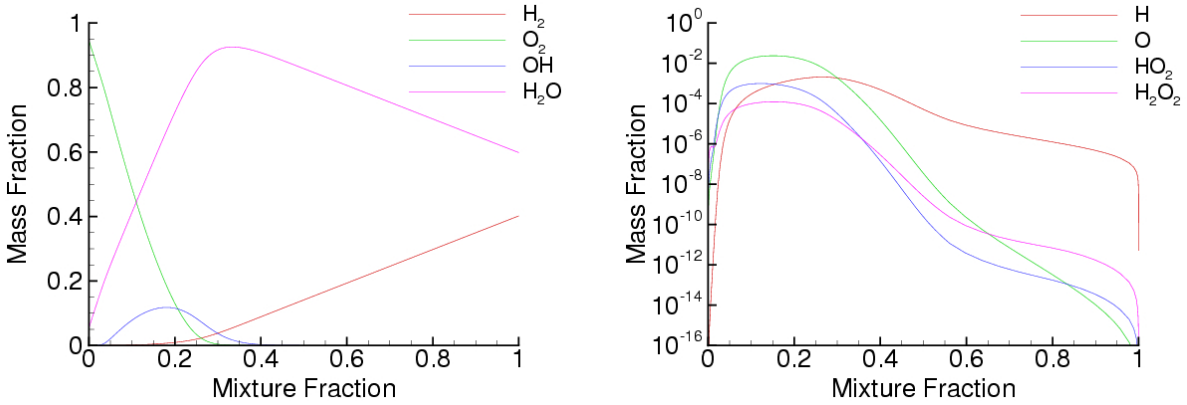

Figure 5: Mass fraction distribution of major (left) and minor (right) species as a function of mixture fraction for a strain-rate of 400 s^{-1}.

3.3 Tabulated Combustion Closure Based on LEM

Turbulent reactive closures that relate the statistics of the chemical species to those of a conserved scalar such as mixture fraction have been moderately successful in modeling turbulence-chemistry interactions. Laminar flamelet modeling, for example, attempts to capture the coupling between turbulence and chemistry by constructing sub-models for the probability-density-function (PDF) of mixture fraction and scalar dissipation rate. The flamelet equations are solved in mixture-fraction coordinates in advance as a pre-processing operation to build the so-called flamelet libraries. Simulations that solve the transport equation for mixture fraction can then use these libraries to estimate temperature and species concentrations. In this way, the number of equations to be solved can be dramatically reduced and stiffness associated with the chemical mechanism is handled in the preprocessing phase.

A current difficulty with the flamelet approach is that it cannot predict local extinction and re-ignition behavior reliably. The primary reason is that the dependence of the scalar dissipation rate, χ, on mixture fraction, F, is not modeled correctly. An alternative that can potentially circumvent this difficulty is the Linear Eddy Model (LEM) of Kerstein (1988-1992). This model solves a one-dimensional reaction-diffusion equation that resolves processes over all the length scales of turbulence and chemistry. Molecular diffusion and reactive source terms are computed explicitly. Advection is modeled by a stochastic mapping procedure that satisfies the three-dimensional inertial range scaling laws. This model also has the potential for improved predictions of pollutant formation.

Here, we have developed a new tabulation approach based on LEM. We show preliminary results that use LEM to build a turbulent library of the thermo-chemical state evolved by reaction, diffusion, and advection at the smallest scales. Unlike past implementations of this model, thermo-chemical state libraries are constructed in a manner directly analogous to the conventional flamelet-library approach (similar to Figs. 4 and 5). A unique difference, however, is that LEM simulates instantaneous realizations of the flow as a function of both the resolved and the unresolved strain-rate imposed by turbulent eddies. Thus, ensemble averaged solutions of the LEM field can be directly parameterized and tabulated based on filtered values of F, χ and the turbulent Reynold's number, Re_L. This eliminates the need to introduce additional models to link filtered quantities with instantaneous quantities.

There are three additional benefits of the tabulated LEM approach. First, the laminar flamelet assumption can be relaxed since the effect of unresolved turbulent eddies and the mean strain rate is included. Second, unsteady effects can be captured in a straight-forward manner since the unsteady reaction-diffusion equations are solved directly. Third, non-unity Lewis number and differential diffusion effects can be captured easily and are accounted for in the tabulation. To test this method, we have applied the model to a variety of flames to test the degree to which experimental results can be reproduced. Here we show results from a preliminary

investigation focused on how well LEM represents simple jet flames of $CH_4/H_2/N_2$. The property evaluation scheme described in section 3.1 was used to account for detailed transport processes.

Model parameters needed for LEM are the integral length scale, L, and Re_L. Two sets of simulations were performed for Re_L= 235 and 360. Figure 6 shows scatter plots of the simulated (left) and measured (right) temperature distribution in mixture fraction space. The LEM implementation produces the correct trends as Re_L is increased. The scatter associated with the peak temperature suggests that some degree of local extinction is being captured by the model. This trend was further investigated by examining the scatter plots of OH mass fraction. These are shown in Fig. 7. The presence of very low quantities of OH mass fraction (~ 0.001) near the stoichiometric mixture fraction clearly indicates local reduction in reaction rates due to the turbulent eddies. Studies are still required to understand the precise mechanism that induces partial extinction and the degree to which the tabulated LEM approach represents this mechanism.

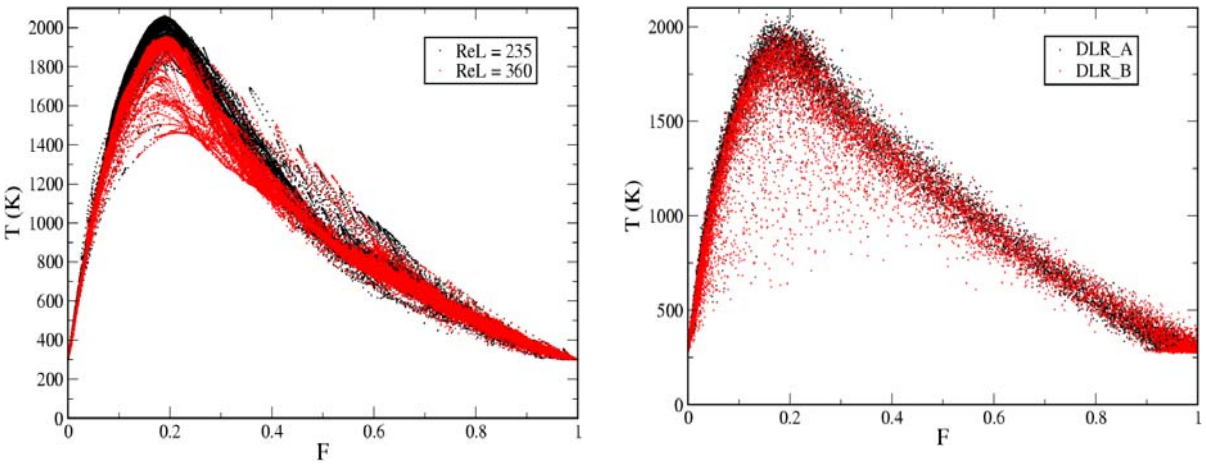

Figure 6: Scatter plots of the simulated (left) and measured (right) temperature versus mixture fraction.

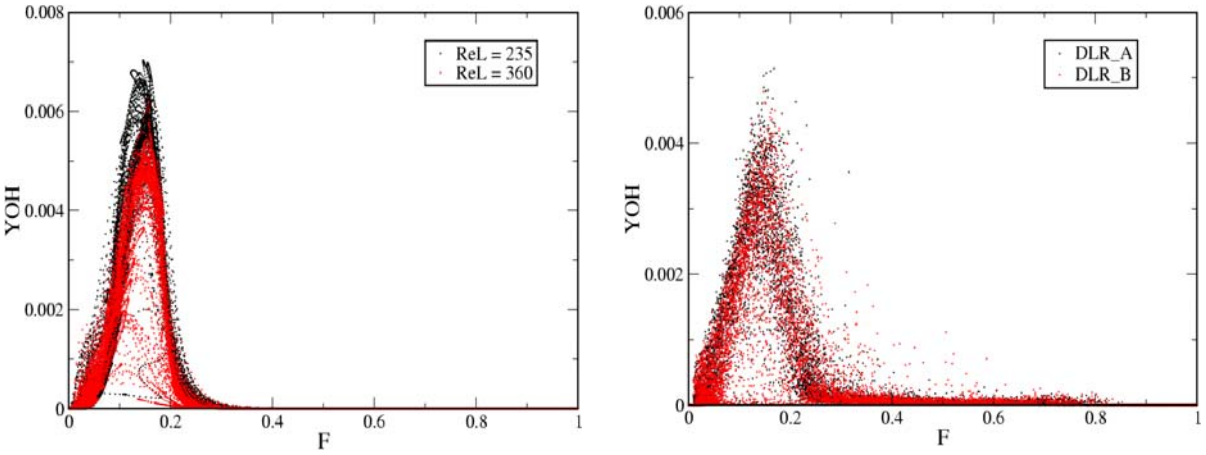

Figure 7: Scatter plots of the simulated (left) and measured (right) OH mass fraction versus mixture fraction.

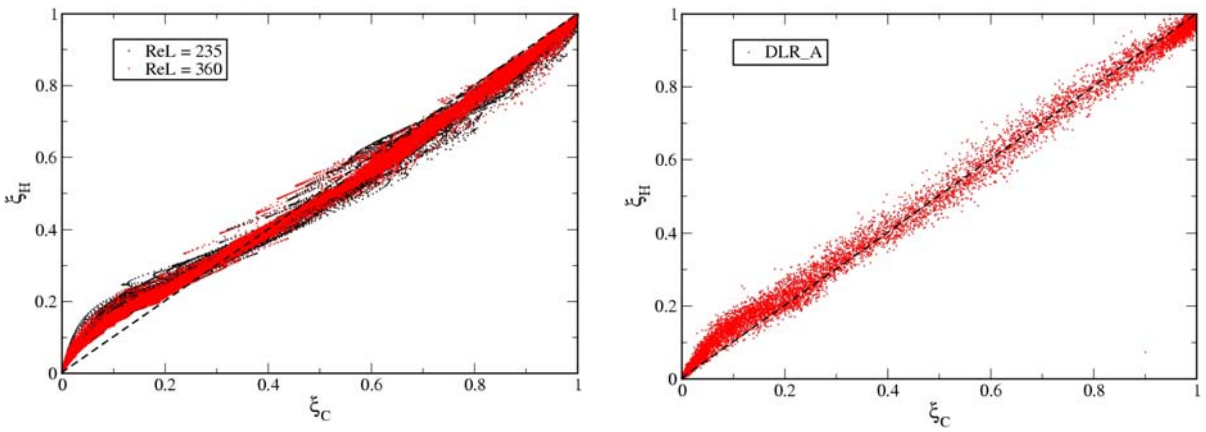

Figure 8: Scatter plots of the simulated (left) and measured (right) elemental carbon mixture fraction versus elemental hydrogen mixture fraction.

To assess the tabulated LEM model's ability to capture differential diffusion effects, plots of the elemental carbon mixture fraction, ξ_C, and elemental hydrogen mixture fraction, ξ_H, are shown in Fig. 8. Both cases show significant differential diffusion. The case with higher Re_L shows a slightly smaller effect compared to lower Re_L. This trend is similar to that seen in the experiments, where differential diffusion effects were found to be higher in the near field of the jet (low turbulence) compared to the downstream location (higher turbulence). These results suggest that the tabulated LEM approach has the potential to capture important physics that other models miss. We are in the process of assessing the models performance as the mean strain rates and Re_L is increased.

4 Conclusions

The coupled model framework described above has been validated for use at the conditions of interest in the CRF optical DI-H2ICE. We have just completed generation of the tabulated LEM libraries using the detailed hydrogen-air kinetics mechanism described in section 3.2 (i.e., O'Conaire et al. 2004). This model has been implemented in a full LES of the optical engine using the grid, valve, and spark timing profiles shown in Figs. 1 and 2. Additionally, we have begun to perform hydrogen fuel injector pattern optimization studies with detailed thermodyamics and transport included in the calculations. Our goals as we move forward are to focus on the critical needs and challenges associated with the use of hydrogen as a fuel. These needs include obtaining a clearer understanding of power density limitations, maximum fuel efficiency, in-cylinder NOX formation, turbulent mixing characteristics, turbulence-chemistry interactions, and the effects of mixture stratification as a function of local in-cylinder processes over full engine cycles.

References

Barlow, R. S. (1996-2006). *International Workshop on Measurement and Computation of Turbulent Nonpremixed Flames*, www.ca.sandia.gov/TNF, Combustion Research Facility, Sandia National Laboratories.

Barlow, R. S. and Frank, J. H. (1998). Effects of Turbulence on Species Mass Fractions in Methane/Air Jet Flames, *Proceedings of the Combustion Institute*, **27**: 1087-1095.

Barlow, R. S., Fiechtner, G. J., Carter, C. D. and Chen, J.-Y. (2000). Experiments on the Structure of Turbulent CO/H2/N2 Jet Flames, *Combustion and Flame*, **120**: 549-569.

Barlow, R. S., Smith, N. S. A., Chen, J.-Y. and Bilger, R. W. (1999). Nitric Oxide Formation in Dilute Hydrogen Jet Flames: Isolation of the Effects of Radiation and Turbulence-Chemistry Submodels, *Combustion and Flame*, **117**: 4-31.

Bird, R. B., Stewart, W. E. and Lightfoot, E. N. (1960). *Transport Phenomena*, John Wiley and Sons, Incorporated, New York, New York.

Cabra, R., Myhrvold, T., Chen, J.-Y., Dibble, R. W., Karpetis, A. N. and Barlow, R. S. (2002). Simultaneous Laser Raman-Rayleigh-LIF Measurements and Numerical Modeling Results of a Lifted Turbulent H2/N2 Jet Flame in a Vitiated Coflow, *Proceedings of the Combustion Institute*, **29**: 1881-1888.

Dally, B. B., Masri, A. R., Barlow, R. S. and Fiechtner, G. J. (1998). Instantaneous and Mean Compositional Structure of Bluff-Body Stabilized Nonpremixed Flames, *Combustion and Flame*, **114**: 119-148.

Ely, J. F. and Hanley, H. J. M. (1981a). Prediction of Transport Properties. 1. Viscosity of Fluids and Mixtures, *Industrial and Engineering Chemistry Fundamentals*, **20**(4): 323-332.

Ely, J. F. and Hanley, H. J. M. (1981b). Prediction of Transport Properties. 2. Thermal Conductivity of Pure Fluids and Mixtures, *Industrial and Engineering Chemistry Fundamentals*, **22**(1): 90-97.

Erlebacher, G., Hussaini, M. Y., Speziale, C. G. and Zang, T. A. (1992). Toward the Large Eddy Simulation of Compressible Turbulent Flows, *Journal of Fluid Mechanics*, **238**: 155-185.

Germano, M., Piomelli, U., Moin, P. and Cabot, W. H. (1991). A Dynamic Subgrid-Scale Eddy Viscosity Model, *Physics of Fluids*, **3**(7): 1760-1765.

Gordon, S. and McBride, B. J. (1971). *Computer Program for Calculation of Complex Chemical Equilibrium Compositions, Rocket Performance, Incident and Reflected Shocks and Chapman-Jouguet Detonations*, Technical Report NASA SP-273, National Aeronautics and Space Administration.

Hirschfelder, J. O., Curtiss, C. F. and Bird, R. B. (1964). *Molecular Theory of Gases and Liquids*, Second Edition, John Wiley and Sons, Incorporated, New York, New York.

Kalt, P. A., Al-Abdeli, Y. M., Masri, A. R. and Barlow, R. S. (2002). Swirling Turbulent Non-Premixed Flames of Methane: Flow Field

and Compositional Structure, *Proceedings of the Combustion Institute*, **29**: 1913-1919.

Kee, R. J., Rupley, F. M. and Miller, J. A. (1990). Chemkin Thermodynamic Data Base, Technical Report SAND87-8215B, Sandia National Laboratories. Supersedes SAND87-8215 dated April 1987.

Kerstein, A. R. (1988). A Linear-Eddy Model of Turbulent Scalar Transport and Mixing. *Combustion Science and Technology*, **60**: 391–421.

Kerstein, A. R. (1989). Linear-Eddy Modeling of Turbulent Transport II: Application to Shear Layer Mixing. *Combustion and Flame*, **75**: 397–413.

Kerstein, A. R. (1990). Linear-Eddy Modeling of Turbulent Transport. Part 3. Mixing and Differential Molecular Diffusion in Round Jets. *Journal of Fluid Mechanics*, **216**: 411–435.

Kerstein, A. R. (1992). Linear-Eddy Modeling of Turbulent Transport. Part 4. Structure of Diffusion Flames. *Combustion Science and Technology*, **81**: 75–96, 1992.

Kerstein, A. R. (1991). Linear-Eddy Modeling of Turbulent Transport. Part V: Geometry of Scalar Interfaces. *Physics of Fluids A*, **3**(5): 1110–1114.

Kerstein, A. R. (1991). Linear-Eddy Modeling of Turbulent Transport. Part 6. Microstructure of Diffusive Scalar Mixing Fields. *Journal of Fluid Mechanics*, **231**: 361–394.

Kerstein, A. R. (1992). Linear-Eddy Modeling of Turbulent Transport. Part 7. Finite-Rate Chemistry and Multi-Stream Mixing. *Journal of Fluid Mechanics*, **240**: 289–313.

Leland, T. W. and Chappelear, P. S. (1968). The Corresponding States Principle. A Review of Current Theory and Practice, *Industrial and Engineering Chemistry Fundamentals*, **60**(7): 15-43.

Lilly, D. K. (1992). A Proposed Modification of the Germano Subgrid-Scale Closure Method, *Physics of Fluids*, **3**(11): 633-635.

Meier, W., Barlow, R. S., Chen, Y.-L. and Chen, J.-Y. (2000). Raman/Rayleigh/LIF Measurements in a Turbulent CH4/H2/N2 Jet Diffusion Flame: Experimental Techniques and Turbulence Chemistry Interaction, *Combustion and Flame*, **123**: 326-343.

Moin, P., Squires, K., Cabot, W. and Lee, S. (1991). A Dynamic Subgrid-Scale Model for Compressible Turbulence and Scalar Transport, *Physics of Fluids*, **3**(11): 2746-2757.

O'Conaire, M., Curran, H. J., Simmie, J. M., Pitz, W. J. and Westbrook, C. K. (2004). A Comprehensive Modeling Study of Hydrogen Oxidation, International Journal of Chemical Kinetics, **36**(11): 603-622.

Oefelein, J. C. (2005). Thermophysical Characteristics of LOX-H2 Flames at Supercritical Pressure, *Proceedings of the Combustion Institute*, **30**: 2929-2937.

Oefelein, J. C. (2006a). Large Eddy Simulation of Swirling Particle-Laden Flow in a Model Axisymmetric Combustor, *Proceedings of the Combustion Institute*, **31**, 2291-2299.

Oefelein, J. C. (2006b). Large Eddy Simulation of Turbulent Combustion Processes in Power and Propulsion Systems (**Invited**), *Progress in Aerospace Sciences*, **42**: 2-37.

Oefelein, J. C. (2006c). Mixing and Combustion of Cryogenic Oxygen-Hydrogen Shear-Coaxial Jet Flames at Supercritical Pressure, *Combustion Science and Technology*, **178**(1-3): 229-252.

Oefelein, J. C., Schefer, R. W. and Barlow, R. W. (2006). Toward Validation of LES for Turbulent Combustion (**Invited**), *AIAA Journal*, **44**(3): 418-433.

Reid, R. C., Prausnitz, J. M. and Polling, B. E. (1987). *The Properties of Liquids and Gases*, Fourth Edition, McGraw-Hill, New York, New York.

Rowlinson, J. S. and Watson, I. D. (1969). The Prediction of the Thermodynamic Properties of Fluids and Fluid Mixtures-I. The Principle of Corresponding States and its Extensions, *Chemical Engineering Science*, **24**(8): 1565-1574.

Segura, J. C., Eaton, J. K. and Oefelein, J. C. (2004). *Predictive Capabilities of Particle-Laden Large Eddy Simulation*, Technical Report TSD-156, Department of Mechanical Engineering, Stanford University Stanford, California.

Smagorinsky, J. (1963). General Circulation Experiments with the Primitive Equations. I. The Basic Experiment, *Monthly Weather Review*, **91**: 99-164.

Speziale, C. G. (1985). Galilean Invariance of Subgrid-Scale Stress Models in the Large Eddy Simulation of Turbulence, *Journal of Fluid Mechanics*, **156**: 55-62.

Takahashi, S. (1974). Preparation of a Generalized Chart for the Diffusion Coefficients of Gases at High Pressures, *Journal of Chemical Engineering of Japan*, **7**(6): 417-420.